

Power Topology – Buck Converter

Mickael Lauer

PMP-DCS DC/DC Controllers

ABSTRACT

This application report shows a general step-by-step, Type-III compensation design procedure for current-mode, step-down dc/dc converters as well as the PMP5532 design example using the Texas Instruments TPS40055 step-down converter integrated circuit.

This report also illustrates how to achieve high efficiency in a step-down converter using a wide-input voltage range. In addition to the Type-III compensation calculation, the report provides the calculations needed to estimate the power losses including an example that achieves up to 95% efficiency.

Contents

1	Introduction	2
2	Compensation Loop Design	2
	2.1 Compensation Networks Basics	2
	2.2 Design Procedure for Current-Mode, Type-III Compensation Networks	3
	2.3 Example	4
3	Efficiency	10
	3.1 Power Dissipated in MOSFETs	11
	3.2 Power Dissipated in Inductor	12
	3.3 Efficiency Calculation Formula	13
	3.4 Example	13
4	Tools	15
5	Conclusion	15

List of Figures

1	TPS40055 Schematic	2
2	Type-III Compensation Schematic.....	2
3	Poles and Zeros Placement for Type-III Compensation	3
4	Theoretical Bode Plot of a Compensation Loop	4
5	TPS40055 Wide V_{IN} Design Schematic	5
6	Compensation Loop Bode Plot – Initial Attempt	7
7	Refined Compensation Loop Bode Plot.....	8
8	Measured Bode Plot With Optimized Compensation Loop	10
9	Nonsynchronous Buck Topology	11
10	I_{rms} Current Formulas for MOSFETs Waveforms	11
11	Current Ripple in the Inductor	12
12	Current Waveform at MOSFETs and Inductor Output – Calculated With Power Stage Designer Software	13
13	Measured Efficiency of PMP5532revB	14

List of Tables

1	PMP5532revB Parameters	4
---	------------------------------	---

SwitcherPro, TPS40K, SWIFT are trademarks of Texas Instruments.
 Mathcad is a trademark of Mathsoft, Inc.
 Excel is a trademark of Microsoft Corporation.

2	PMP5532revB Bill Of Materials	5
3	First Compensation Loop Calculation	6
4	Final Optimized Pole and Zero Frequencies	9
5	PMP5532revB Parameters	13
6	Comparison of Measured and Estimated Efficiency	14
7	Major Sources of Power Losses in Buck Design	14

1 Introduction

The two most commonly used figures of merit for power supplies are efficiency and transient response. Optimizing these two parameters requires proper estimation of the power losses and, usually, the adoption of Type-III compensation to boost the crossover frequency and phase margin. This exercise is made more complex when the voltage translation is large, i.e., from a high-input voltage to a low-output voltage.

This document shows a general, step-by-step calculation and fine tuning of Type-III compensation design for a current-mode, step-down dc/dc converter as well as the TPS4005x from the TI portfolio. Then, it explains how to calculate the dissipated power to reach a high efficiency (up to 95%).

The TPS4005x is a family of high-voltage, wide-input (8 V to 40 V), synchronous, step-down controllers. It offers design flexibility with a number of useful features such as:

- Input voltage feed forward
- Programmable fixed-frequency, voltage-mode operation
- Externally synchronizable
- Programmable, closed-loop soft start

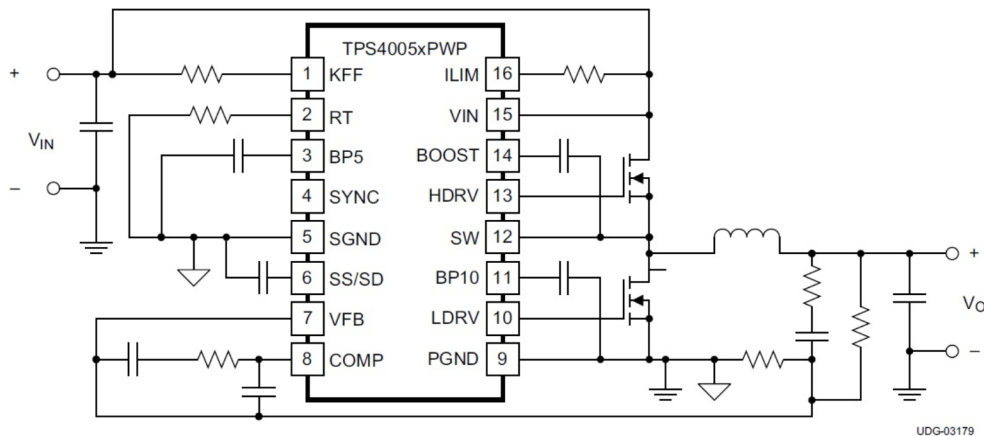


Figure 1. TPS40055 Schematic

2 Compensation Loop Design

2.1 Compensation Networks Basics

It is possible to improve the transient response of a current-mode dc/dc converter by replacing a Type-II compensation scheme with a Type-III to boost the crossover frequency and phase margin. Type-III compensation is simple to design and needs only two extra components compared to a classic Type-II compensation. Figure 2 shows the commonly used theoretical Bode plot of Type-III compensation. The particular poles and zeros are detailed with the respective formulas in Figure 3.

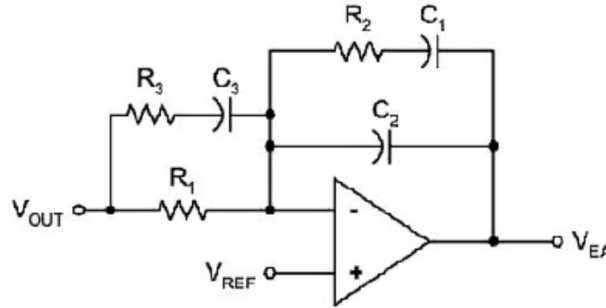
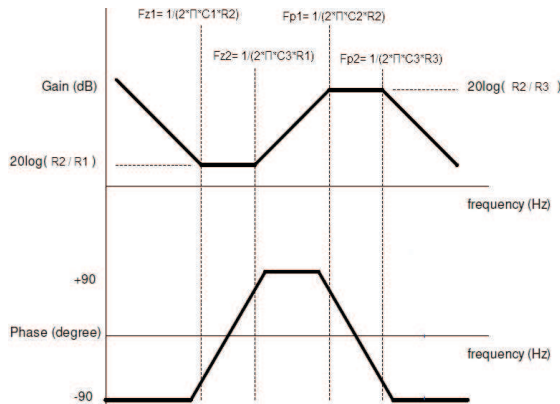


Figure 2. Type-III Compensation Schematic



$f_{z1} \approx \frac{1}{2 \times \pi \times C1 \times R2}$	$f_{z2} \approx \frac{1}{2 \times \pi \times C3 \times R1}$
$f_{p1} \approx \frac{1}{2 \times \pi \times C2 \times R2}$	$f_{p2} \approx \frac{1}{2 \times \pi \times C3 \times R3}$

Figure 3. Poles and Zeros Placement for Type-III Compensation

2.2 Design Procedure for Current-Mode, Type-III Compensation Networks

A Type-III compensation loop comprises two poles and two zeros.

The compensation network needs to be calculated and tested in detail to achieve a stable system with high bandwidth. Switching power supplies are sampled-data systems. A step-down converter is only limited in bandwidth by the switching frequency. The Nyquist frequency (which is half the switching frequency) is the absolute limit of information transfer, but it is impossible to cross over a loop as high as this. That is why it is a good practice to try to reach a crossover frequency of one-fifth of the switching frequency, f_{sw} .

For a stable system, a good practice is to target a phase margin of 60° at the crossover frequency, or preferably, a little bit more if the output capacitors are not a ceramic type (because an electrolytic type undergoes an ESR (equivalent series resistance) increase due to aging effects).

To achieve the goal of stability, it is necessary to dimension the compensation loop with an initial calculation:

1. Place the first zero (f_{z1}) before the resonant frequency.

$$\left(\text{due to the output resonant circuit } f_{res} = \frac{1}{2 \times \pi \times \sqrt{L} \times C_{out}} \right)$$

2. Place the second zero (f_{z2}) around the resonant frequency (the lower the zero frequency is, the better the phase margin at the expense of closed-loop performance).
3. Place the first pole (f_{p1}) around the crossover frequency, just after the ESR zero.
4. Place the second pole (f_{p2}) just after the ESR zero or at half the switching frequency.

Now, plot the result of the compensation loop in a Bode diagram, including the power stage, and add the two curves as shown in [Figure 4](#).

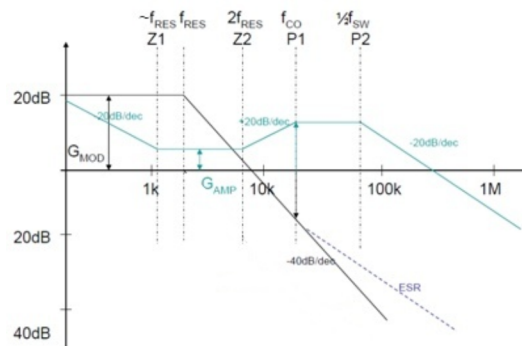


Figure 4. Theoretical Bode Plot of a Compensation Loop

These steps give a first solution that the designer usually has to fine-tune and improve the bandwidth and phase margin.

The compensation gain has to be lower than the open-loop gain of the error amplifier, because the error amplifier cannot react faster than its open-loop gain. Once the gain and phase plots are measured, the system most probably needs some adjustment due to parasitic effects of the board and components that have not been part of the calculation.

Adjust step by step the poles and/or zeros in order to shape the gain profile and ensure that the phase margin is greater than 45° . The first parameter to lock is the stability of the system. At the crossover frequency it is a good practice to have a phase margin higher than 45° ; 60° is what is generally targeted.

Once this goal is achieved, most of the time the f_{CO} frequency can be improved. Typically, it is just necessary to adjust the compensation loop gain by changing the right resistance values (in this design R2). Increasing the gain has the effect of increasing the f_{CO} and vice versa. The complete process of adjusting poles, zeros, and gain is explained in the [Section 2.3](#).

2.3 Example

2.3.1 Design Description

Based on the PMP5532revB standard board for the TPS40055, the following example demonstrates how to achieve high bandwidth with good phase margin (to ensure system stability), and also how to design a solution with high efficiency.

The following parameters ([Table 1](#)) for the TPS40055 are assumed in this document.

Table 1. PMP5532revB Parameters

Parameters	Value
Output voltage (V_{OUT})	3.3 V
Output current (I_{OUT})	6 A
Input voltage (V_{IN})	22 V to 30 V with nominal voltage of 28 V
Switching frequency (f_{SW})	100 kHz

Figure 5 provides the schematic of the PMP5532revB:

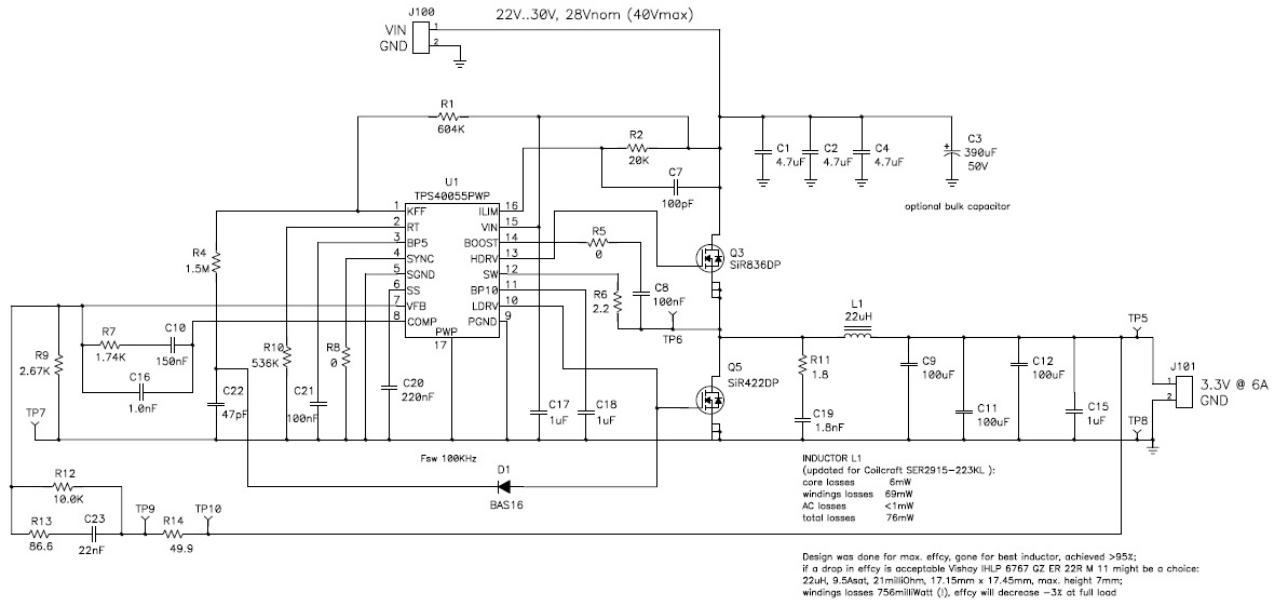


Figure 5. TPS40055 Wide V_{IN} Design Schematic

Table 2 shows the complete bill of materials for the PMP5532revB.

Table 2. PMP5532revB Bill Of Materials

Count	RefDes	Value	Description	Size	Part Number	MFR
3	C1	4.7 μ F	Capacitor, Ceramic, 4.7 μ F, 50V, X7R, 15%	1210	C3225X7R1H475M	TDK
	C2	4.7 μ F	Capacitor, Ceramic, 4.7 μ F, 50V, X7R, 15%	1210	C3225X7R1H475M	TDK
1	C3	390 μ F	Capacitor, Aluminum, SM, 5-V, 80-milliohms (FC series)	16 x 15 mm	EEUF1H391S	Panasonic
	C4	4.7 μ F	Capacitor, Ceramic, 4.7 μ F, 50V, X7R, 15%	1210	C3225X7R1H475M	TDK
1	C7	100 pF	Capacitor, Ceramic, 100 pF, 50 V, NPO, 10%	0603	Std	Std
1	C8	100 nF	Capacitor, Ceramic, 100 nF, 25 V, X7R, 10%	0805	Std	Std
3	C9	100 μ F	Capacitor, Ceramic, 6.3V, 15%, X5R	1210	C3225X5R0J107M	TDK
1	C10	150 nF	Capacitor, Ceramic, 150 nF, 25 V, X7R, 10%	0603	Std	Std
	C11	100 μ F	Capacitor, Ceramic, 6.3 V, 15%, X5R	1210	C3223X5R0J107M	TDK
	C12	100 μ F	Capacitor, Ceramic, 6.3 V, 15%, X5R	1210	C3223X5R0J107M	TDK
1	C15	1 μ F	Capacitor, Ceramic, 1 μ F, 16 V, X7R, 15%	0603	Std	Std
1	C16	1.0 nF	Capacitor, Ceramic, 10 nF, 50 V, X7R, 10%	0603	Std	Std
1	C17	1 μ F	Capacitor, Ceramic, 1 μ F, 50 V, X7R, 10%	1206	Std	Std
1	C18	1 μ F	Capacitor, Ceramic, 1 μ F, 16 V, X7R, 10%	1206	Std	Std
1	C19	1.8 nF	Capacitor, Ceramic, 1.8 nF, 50 V, X7R, 10%	0805	Std	Std
1	C20	220 nF	Capacitor, Ceramic, 0.022 μ F, 50 V, X7R, 10%	0603	Std	Std
1	C21	100 nF	Capacitor, Ceramic, 100 nF, 10 V, X7R, 10%	0603	Std	Std
1	C22	47 pF	Capacitor, Ceramic, 47 pF, 50 V, NPO, 10%	0603	Std	Std
1	C23	22 nF	Capacitor, Ceramic, 22 nF, 50 V, X7R, 10%	0603	Std	Std
1	D1	BAS16	Diode, Switching, 150-mA, 75-V, 350 mW	SOT23	BAS16	Vishay-Liteon
2	J100		Terminal Block, 2-pin, 15-A, 5.1 mm	0.40 x 0.35"	ED1609	OST
	D101		Terminal Block, 2-pin, 15-A, 5.1 mm	0.40 x 0.35"	ED1609	OST
1	L1	22 μ H	Inductor, SMT Power, 8.6Asat, 2.05 milliohm	1.100 x 1.100 inch	SER2915H-223KL	Coilcraft
1	Q3	SiR836DP	MOSFET, N-ch, 40 V, 8.5 A, 22.5 milliohm	PWRPAK S0-8	SiR836DP	Vishay
1	Q5	SiR422DP	MOSFET, N-ch, 40 V, 16 A, 8 milliohm	PWRPAK S0-8	SiR422DP	Vishay
1	R1	604K	Resistor, Chip, 604 k Ω , 1/16-W, 1%	0603	Std	Std
1	R2	20K	Resistor, Chip, 20 k Ω , 1/16-W, 1%	0603	Std	Std
1	R4	1.5M	Resistor, Chip, 1.5 k Ω , 1/16-W, 1%	0603	Std	Std

Table 2. PMP5532revB Bill Of Materials (continued)

Count	RefDes	Value	Description	Size	Part Number	MFR
1	R5	0	Resistor, Chip, 0 Ω, 1/8-W, 5%	0805	Std	Std
1	R6	2.2	Resistor, Chip, 0 Ω, 1/8-W, 5%	0805	Std	Std
1	R7	1.74K	Resistor, Chip, 1.74 kΩ, 1/16-W, 1%	0603	Std	Std
1	R8	0	Resistor, Chip, 0 kΩ, 1/16-W, 1%	0603	Std	Std
1	R9	2.67K	Resistor, Chip, 2.67 kΩ, 1/16-W, 1%	0603	Std	Std
1	R10	536K	Resistor, Chip, 536 kΩ, 1/16-W, 1%	0603	Std	Std
1	R11	1.8	Resistor, Chip, 18 Ω, 1/4-W, 5%	1206	Std	Std
1	R12	10.0K	Resistor, Chip, 10 kΩ, 1/16-W, 1%	0603	Std	Std
1	R13	86.6	Resistor, Chip, 604 Ω, 1/16-W, 1%	0603	Std	Std
1	R14	49.9	Resistor, Chip, 49.9 Ω, 1/16-W, 1%	0603	Std	Std
4	TP5		Test Point, Red, 1 mm	0.038"	240-345	Farnell
	TP6		Test Point, Red, 1 mm	0.038"	240-345	Farnell
2	TP7		Test Point, Black, 1 mm	0.038"	240-333	Farnell
	TP8		Test Point, Black, 1 mm	0.038"	240-333	Farnell
	TP9		Test Point, Red, 1 mm	0.038"	240-345	Farnell
	TP10		Test Point, Red, 1 mm	0.038"	240-345	Farnell
1	U1	TPS40055PWP	IC, Wide Input Synchronous Buck Controller	PWP16	TPS40051PWP	Texas Instruments

Notes: 1. These assemblies are ESD sensitive, ESD precautions shall be observed.
 2. These assemblies must be clean and free from flux and all contaminants. Use of no clean flux is not acceptable.
 3. These assemblies must comply with workmanship standards IPC-A-610 Class 2.
 4. Ref designators marked with an asterisk (**) cannot be substituted. All other components can be substituted with equivalent MFG's components.

2.3.2 First Compensation Loop Calculation

According to the requirements given in [Section 2.2](#), values of pole and zero frequencies in [Table 4](#) are selected, f_{z1} , f_{z2} , respectively, and placed before and around the resonance frequency. Pole frequencies f_{p1} , f_{p2} are placed around the crossover frequency and at half of the switching frequency. The gain and R1 are fixed arbitrarily to reduce the degrees of freedom. Then, the gain is thereafter fine-tuned to improve the crossover frequency. The full details to calculate the right components (resistance and capacitor) are giving in [Section 2.3.4](#).

Table 3. First Compensation Loop Calculation

$f_{z1} = 1.2 \text{ kHz}$	$f_{z2} = 3 \text{ kHz}$	$f_{p1} = 20 \text{ kHz}$	$f_{p2} = 50 \text{ kHz}$	Gain: 0.4/-7.95 dB	
	$R2 = G \times R1$	$R3 = \frac{1}{2 \times \pi \times C3 \times Fp2}$	$C1 = \frac{1}{2 \times \pi \times R2 \times Fz1}$	$C2 = \frac{1}{2 \times \pi \times R2 \times Fp1}$	$C3 = \frac{1}{2 \times \pi \times R1 \times Fz2}$
R1 = 10 kΩ	R2 = 4.0 kΩ	R3 = 640 Ω	C1 = 33 nF	C2 = 2 nF	C3 = 5 nF

Figure 6 shows the Bode gain and phase plots for the complete system including the error amplifier open loop: gain (dark purple), the power stage (gain: red and phase: blue), the compensation (names total; gain black and phase: black and thin).

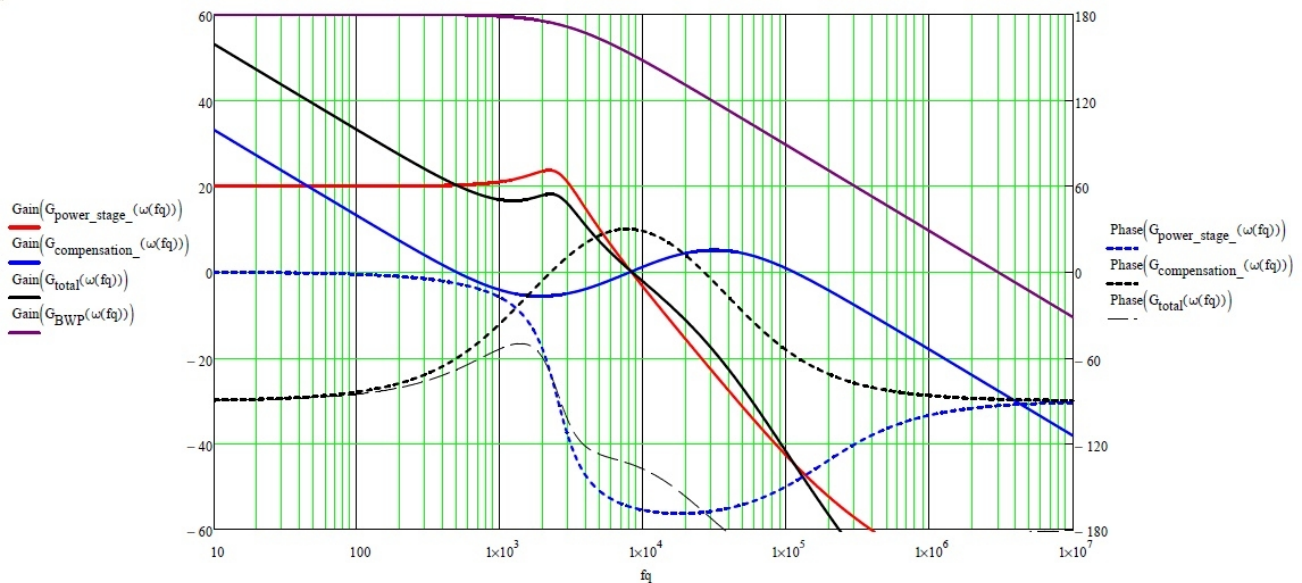


Figure 6. Compensation Loop Bode Plot – Initial Attempt

This first estimation achieves a poor crossover frequency of 8.34 kHz with an acceptable phase margin at the practical limit for production stability of 45.63°. It proves that the foregoing requirements are not a perfect design method, but some empirical rules are useful for the first step in pole and zero placements.

After this first step, the designer has to optimize the location of each pole and zero frequency to adjust the compensation loop gain to achieve the highest crossover frequency with a comfortable phase margin (around 60°). This is explained in the following paragraphs.

NOTE: Figure 4 was also a theoretical plot; the frequencies behavior illustrated in that figure is not as accurate as that observable in Figure 6.

2.3.3 Second Step: Adjusting Pole and Zero Frequencies

After first deriving a tentative stable system, the designer can now fine-tune the pole and zero frequencies by several approaches and simulations. As no specific rules apply, this work can be done with an Excel™ or Mathcad™ sheet. The second simulation has been done with this fine-tune procedure to increase the f_{CO} with a double pole, double zero (in order to simplify the calculations and improve the phase margin):

- 1/50 of f_{SW} for the two zeros, so $F_{z1} \approx F_{z2} \approx 2$ kHz
- Poles around the f_{SE} , so $F_{p1} \approx F_{p2} \approx 90$ kHz
- Gain reduced at 0.6 dB or 1.07 linear

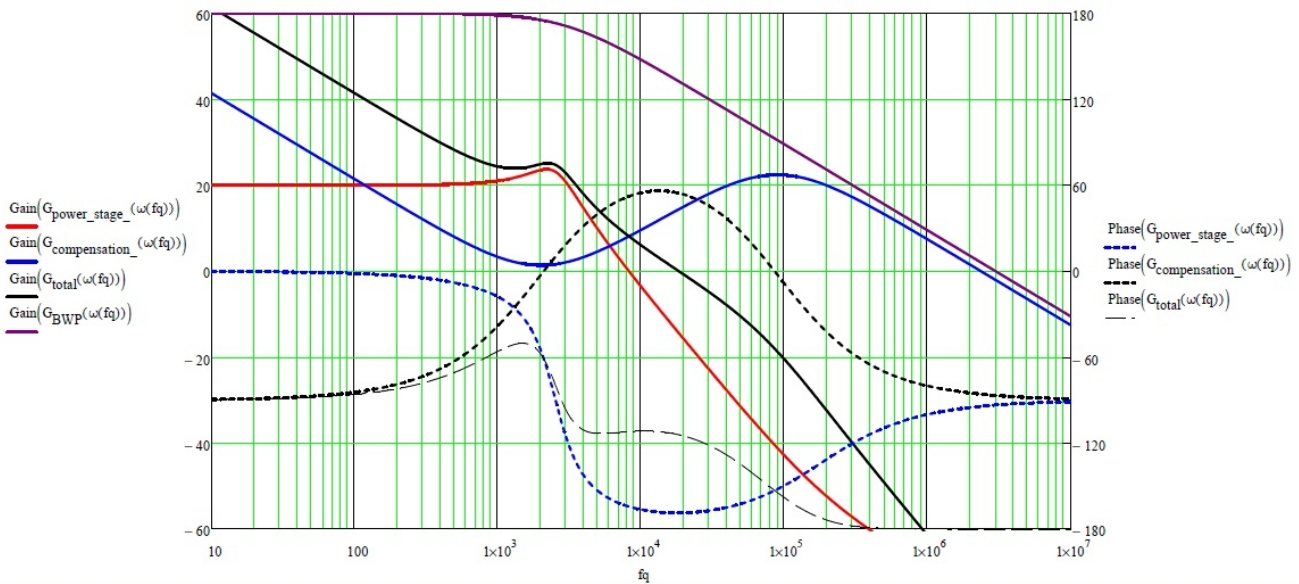


Figure 7. Refined Compensation Loop Bode Plot

It is also necessary to set the compensation loop gain in order to calculate the different compensation components. The limitation for the gain is to not cross the error amplifier gain bandwidth limit (in purple). With these new values, f_{CO} has been improved to 18.41 kHz at 66° phase margin. By only changing the gain (changing R2 resistance), the compensation curve only moves vertically as an offset. It is a mean to adjust the crossover frequency: for example if the crossover frequency is too low, the gain can be increased to reach a higher frequency as explained in [Section 2.2](#).

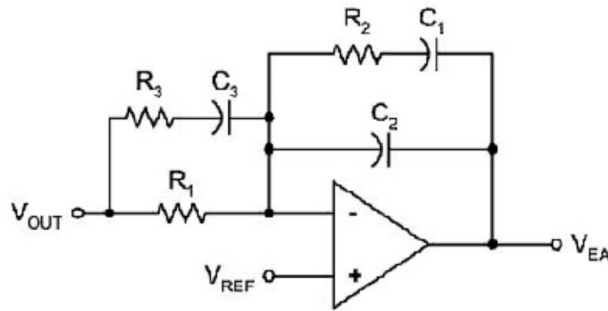
2.3.4 Third Step: Fine Tuning

The following calculations are the ones finally used to achieve the theoretical maximum crossover frequency of 20 kHz. These values have been found after theoretical adjustment of the poles and zeros and compensation loop gain. But it is also recommended to implement the hardware board and make measurements as soon as the design is stable with a reasonable f_{CO} ($1/10$ of f_{sw}). In fact, the hardware world is not perfect and due to multiple parasitic effects, simulations and real measurements are not the same most of the time. Although not achieving the perfect simulation model, start the hardware measurements at the same time in the global design process. In this case, the following frequencies ([Table 5](#)) have been fine-tuned by f_{CO} and phase margin hardware measurements after the second step assumptions.

To reduce the degrees of freedom in the design, it is necessary to set some values as was assumed previously. Set the gain and the resistor R1; the value of R1 is somewhat arbitrary, but this value influences other component values:

- Gain at 0.174 (or -15.18 dB)
- R1 at 10 k Ω
- Reduced zeros frequencies less than 1 kHz
- Keep pole frequencies around 90 kHz

Then, it is possible to calculate all other component values related to the compensation loop, as the following equations demonstrate. For convenience, the illustration of the Type-III compensation schematic also follows.



NOTE: The values given in parenthesis are the real component values, according to the available standard values. This limitation brings some difference to the desired poles and zeros in [Figure 5](#).

Calculation of R2:

$$G = \frac{R2}{R1}, \text{ so } R2 = G \times R1$$

$$R2 = 0.174 \times 10000 = 1740 \Omega$$

Calculation of C2:

$$f_{p1} \approx \frac{1}{2 \pi \times C2 \times R2}, \text{ so } C2 = \frac{1}{2 \pi \times R2 \times f_{p1}}$$

$$C2 = \frac{1}{2 \pi \times 1740 \times 92000} = 0.99 \text{ nF}(1\text{nF})$$

Calculation of C3:

$$f_{z2} \approx \frac{1}{2 \pi \times C3 \times R1}, \text{ so } C3 = \frac{1}{2 \pi \times R1 \times f_{z2}}$$

$$C3 = \frac{1}{2 \pi \times 10000 \times 700} = 22.73 \text{ nF}(22\text{nF})$$

Calculation of C1:

$$f_{z1} \approx \frac{1}{2 \pi \times C1 \times R2}, \text{ so } C1 = \frac{1}{2 \pi \times R2 \times f_{z1}}$$

$$C1 = \frac{1}{2 \pi \times 1740 \times 600} = 0.15 \text{ nF}(0.15\mu\text{F})$$

Calculation of R3:

$$f_{p1} \approx \frac{1}{2 \pi \times C3 \times R3}, \text{ so } R3 = \frac{1}{2 \pi \times C3 \times f_{p1}}$$

$$R3 = \frac{1}{2 \pi \times 22 \times 10^{-9} \times 83000} = 87.2 \Omega(87\Omega)$$

Table 4. Final Optimized Pole and Zero Frequencies

$f_{z1} = 610 \text{ Hz}$	$f_{z2} = 723 \text{ Hz}$	$f_{p1} = 91.468 \text{ kHz}$	$f_{p2} = 83.537 \text{ kHz}$	Gain: 0.174/-15.19 dB
---------------------------	---------------------------	-------------------------------	-------------------------------	-----------------------

Figure 8 shows the measured Bode plot of the real circuit implemented on the PMP5532 board. A noticeable point is the crossing of the gain curve (red) and 0 dB which is the crossover frequency f_{CO} . Here, f_{CO} is 20 kHz perfectly equal to one-fifth of the switching frequency (100 kHz). At this frequency, the system is also stable with a phase margin of 60° . However, the simulation achieves a crossover frequency of 15.08 kHz at a phase margin of 76.4° . This is a good example that shows the difference between simulation and real world. As previously explained, simulation can help to derive a first stable system; however, for fine-tuning it is necessary to make real measurements on hardware.

Another important point to check is the slope around f_{CO} (-1 , i.e., -20 dB/dec), the gain margin of -10.86 dB is also reasonable. Gain margin is the amount of gain necessary to move the 0-dB crossing to occur at the same frequency as the -180° crossing. The gain margin is the gain on the Bode diagram at the frequency where the phase plot crosses 0° or -180° .

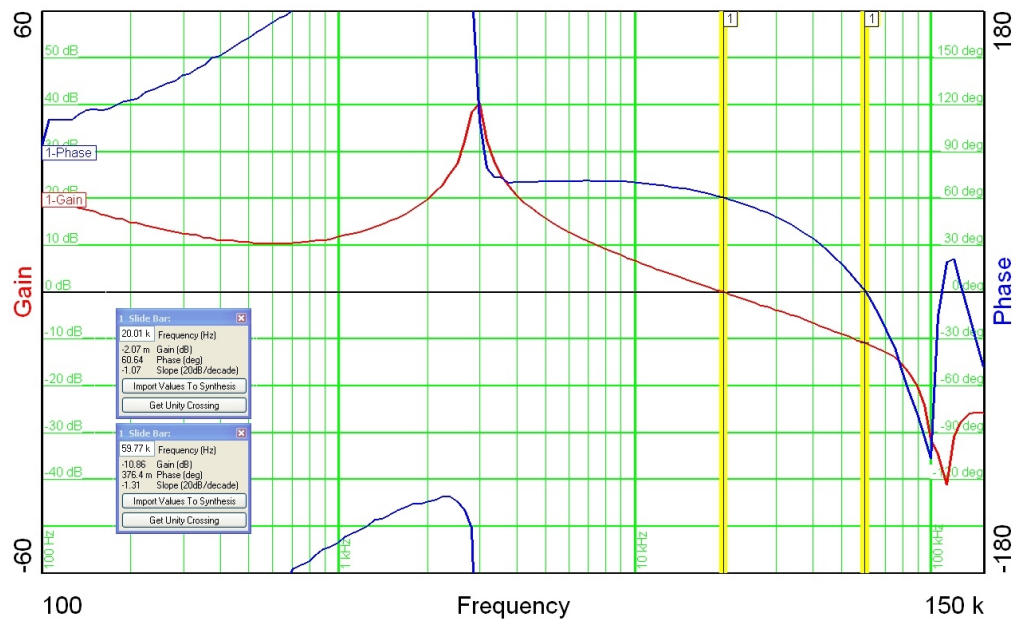


Figure 8. Measured Bode Plot With Optimized Compensation Loop

3 Efficiency

As previously mentioned, the estimation of efficiency is an important part of power supply design. The three main places of power dissipation in a dc-dc converter are:

- MOSFET switching losses (influenced by the turnon and turnoff times of the MOSFETs)
- MOSFET conduction losses (directly proportional to the $r_{DS(on)}$ of the MOSFETs)
- Inductor conduction losses
 - *Core losses*: Energy loss due to the changing magnetic energy in the core during a switching cycle equals the difference between magnetic energy put into the core during the on-time and the magnetic energy extracted from the core during the off-time.
 - *Winding losses*: Power loss in the windings at dc is due to the windings dc resistance and the RMS current through the inductor.

For a greater accuracy, it is also possible to include the MOSFET gate charge losses and body diode dissipation, but in this design these are negligible compared to the three losses just mentioned and can be ignored in most cases.

3.1 Power Dissipated in MOSFETs

To improve efficiency, the rectifier diode CR1 can be replaced by a rectifier MOSFET (see Figure 9). If this is the case, the traditional buck power stage becomes a synchronous buck power stage. In this power stage, an active switch such as another power MOSFET, Q2 in this example, replaces the rectifier, CR1. The rectifier MOSFET is then selected so that its ON voltage drop is less than the forward drop of the rectifier, thus increasing efficiency. Although this complicates the drive circuit design, the gain in efficiency often makes this an attractive option. Other considerations unique to the synchronous buck power stage are preventing cross-conduction and reverse recovery of the parasitic PN diode internal to a MOSFET.

The second MOSFET Q1, shown in Figure 9, plays the role of a switch between the input and the output and is called the high-side MOSFET.

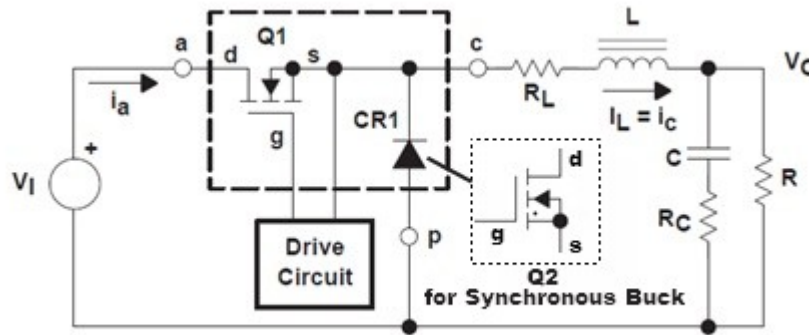


Figure 9. Nonsynchronous Buck Topology

Figure 10 provides the formulas to calculate the RMS current in the high-side and rectifier MOSFETs according to the particular waveforms of the current.

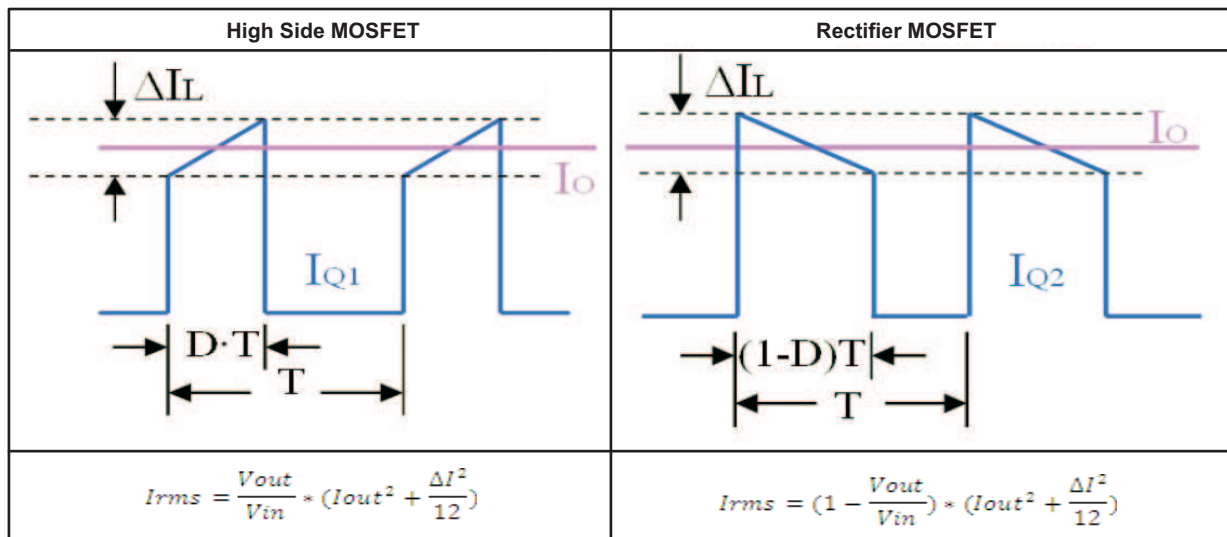


Figure 10. I_{rms} Current Formulas for MOSFETs Waveforms

With the RMS current, it is possible to calculate the total losses in each MOSFET.

3.1.1 Power Dissipated in High-Side MOSFET

The following losses formulas are simplified; they are not fully accurate but accurate enough for good estimations of design losses.

- Conduction losses

$$P_{\text{cond}} = I_{\text{rms2}} \times r_{\text{DS(on)}}$$

$r_{\text{DS(on)}}$ is the on-time, drain-to-source resistance of the high-side MOSFET

- Switching losses

$$P_{\text{sw}} = V_{\text{in}} \times f_{\text{sw}} \times I_{\text{out}} \times (t_f + t_r)$$

Where f_{sw} is the switching frequency of the IC, t_f and t_r are respectively the falling and rising time of the MOSFET.

- Gate charge losses

$$P_{\text{qg}} = Q_g \times V_{\text{gate}} \times f_{\text{sw}}$$

Where Q_g is the MOSFET gate charge and V_{gate} is the gate to source voltage.

The total power loss is the sum of all foregoing power losses:

$$P_{\text{fet}} = P_{\text{sw}} + P_{\text{cond}} + P_{\text{qg}}$$

3.1.2 Power Dissipated in Rectified MOSFET

- Conduction losses

$$P_{\text{cond}} = I_{\text{rms2}} \times r_{\text{DS(on)}}$$

$r_{\text{DS(on)}}$ is the on-time, drain-to-source resistance of the high-side MOSFET.

- Body diode losses

$$P_{\text{bd}} = I_{\text{out}} \times V_{\text{bd}} \times f_{\text{sw}} \times t_{\text{DELAY}}$$

Where f_{sw} is the switching frequency of the IC, V_{DC} is the body diode forward voltage; t_{DELAY} is the delay time just before the SW node rises.

- QG losses

$$P_{\text{qg}} = Q_g \times V_{\text{gate}} \times f_{\text{sw}}$$

Where Q_g is the MOSFET gate charge.

The total power loss is the sum of all power losses:

$$P_{\text{fet}} = P_{\text{sw}} + P_{\text{bd}} + P_{\text{qg}}$$

No switching losses occur on the rectifier side because when the high-side MOSFET turns off, the rectifier is also off. It is not possible to directly turn on the rectifier side without any delay. At this moment, no current flows through the rectifier; only the body diode of the FET creates a voltage and generates body diode losses.

3.2 Power Dissipated in Inductor

Figure 11 shows the current ripple in the inductor with the average value I_{OUT} :

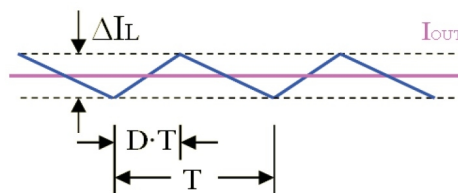


Figure 11. Current Ripple in the Inductor

$$I_{\text{rms}} = I_{\text{out}} + \frac{\Delta I^2}{12}$$

- Core losses

$$P_c = K \times f^x \times B^y \times V_e$$

Where:

K = Constant of core material

f = Frequency in kHz

B = Peak flux density in Tesla

x = Frequency exponent

y = Flux density exponent

V_e = Effective core volume (cm^3)

Core losses are quite complex to estimate, but inductor suppliers (such as Coilcraft) propose

automated calculations on their Web sites.

- Winding losses
 $P_{sw} = I_{rms2} \times DCR$
 Where DCR is the dc resistance of the inductor.

The total power losses are the sum of all power losses:

$$P_{ind} = P_c + P_w + P_{acr}$$

3.3 Efficiency Calculation Formula

Finally, efficiency can be estimated using the following ratio:

$$\eta = \frac{P_{out}}{P_{out} + P_I}$$

With the following assumptions:

$$P_{out} = I_{out} \times V_{out}$$

$P_I = P_{fet} + P_{ind}$ which are the total losses of the design.

3.4 Example

Based on the PMP5532reB standard board for the TPS40055, the following example illustrates how to design a solution with high efficiency.

Assume the parameters listed in (Table 5) for this design.

Table 5. PMP5532revB Parameters

Parameters	Value
Output voltage (V_{OUT})	3.3 V
Output current (I_{OUT})	6 A
Input voltage (V_{IN})	22 V to 30 V and nominal voltage of 28 V
Switching frequency (f_{SW})	100 kHz

In order to calculate the RMS current, it is necessary to know the current waveform at the rectifier, high-side MOSFETs, and inductor. Figure 12 shows the true different waveforms of these components, which were generated by using the Power Stage Designer tool.

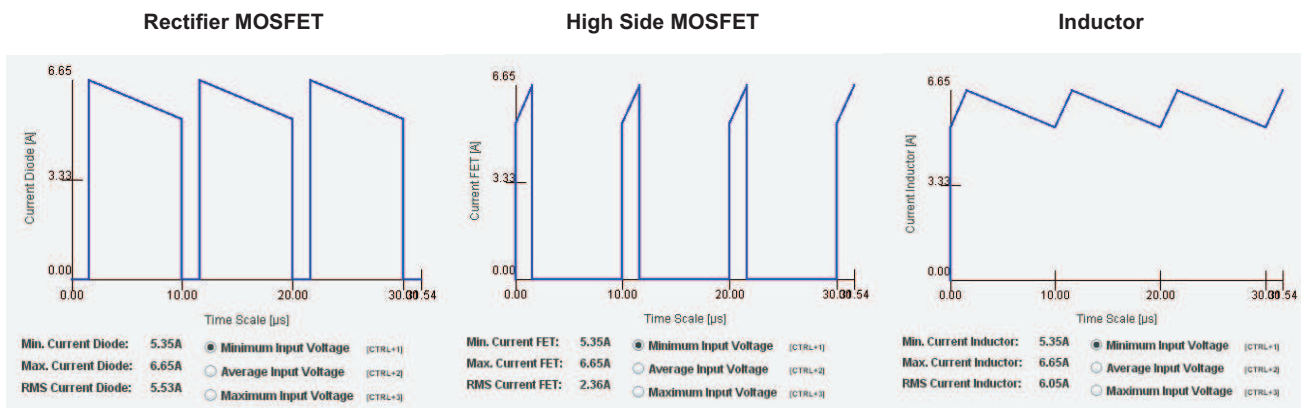


Figure 12. Current Waveform at MOSFETs and Inductor Output – Calculated With Power Stage Designer Software

By applying the previous formulas for losses, the estimated efficiency is 96.3%. Table 6 shows the true efficiency of the design.

Table 6. Comparison of Measured and Estimated Efficiency

Estimated Efficiency	Measured Efficiency	Delta
96.3%	95.3%	1%

Figure 13 shows the measured efficiency on the PMP5532revB board at three different input voltages.

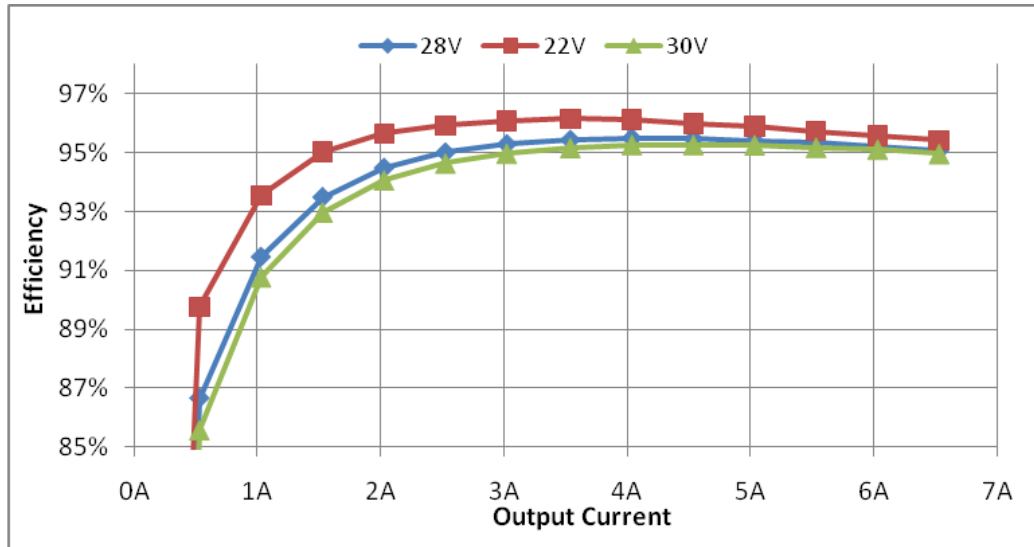


Figure 13. Measured Efficiency of PMP5532revB

According to choice and quality of the Coilcraft inductor and Vishay MOSFETs used, it is possible to reach an efficiency of up to 95%.

- The first choice of the inductor influence on two types of losses: the SER2900 family from Coilcraft offer excellent performances at low switching frequencies due to low DCR. The quality of the inductor also brings the benefit of having a steady efficiency with output current increase (visible in Figure 13 with the efficiency tray between 2 A and 6.5 A).
- The design also has been improved by choosing two Vishay MOSFETs with low $r_{DS(on)}$ and optimized gate/body diode characteristics.

NOTE: A diode in parallel to the rectifier MOSFET also has been added to the design resulting in two following benefits.

- Reduces the power losses due to rectifier body diode (the two MOSFETs cannot switch at the same time)
- Reduces EMI and ringing

The sources of losses for this design are shown in Table 7.

Table 7. Major Sources of Power Losses in Buck Design

Components	Type of Losses	Percentage (%) of Total Losses
High-Side MOSFET		76
	Switching	60
	Conduction	15
	Gate	<1
Rectifier MOSFET		13
	Conduction	5.5
	Body Diode	7.3
	Gate	<1
Inductor		11

Table 7. Major Sources of Power Losses in Buck Design (continued)

Components	Type of Losses	Percentage (%) of Total Losses
	Winding	10.4
	Core	0.6

For this design, losses are mainly generated by high-side switching, which can be improved by finding a low switching gate charge MOSFET. The conduction losses are reasonable due to a choice of good MOSFETs with a low $r_{ds(on)}$. Winding losses also are optimized due to low DCR inductor.

To summarize, for the selection of an inductor and MOSFETs, the important parameters are:

- Low $r_{DS(on)}$ of the rectifier MOSFET
- Short rise and fall times for the high-side MOSFET (linked to gate charge)
- Low dc resistance of the inductor

The best choice for this design are MOSFETs with low $r_{DS(on)}$, V_{DS} of 40 V and SO8 package. At the moment, the high-performance MOSFETs are the following:

- Infineon Optimos series
- Vishay SiR series

4 Tools

The following free, software tools were used to design the example (PMP5532 board) described in this application report:

- **TI Power Stage Designer** is a tool made by design engineers for design engineers. All the calculations to determine voltage and current stress for semiconductors and magnetics inside various topologies are implemented in a single design.
To get this Java application, send an email request to powerstagedesigner@ti.com.
- **SwitcherPro™** is design software that allows you to design and simulate power supplies with Texas Instruments TPS40K™ controllers, low-power dc/dc converters, and SWIFT™ (TPS54xxx) point-of-load, step-down dc/dc products. The Web link is <http://focus.ti.com/docs/toolsw/folders/print/switcherpro.html>.

5 Conclusion

This application report shows an easy way to implement a Type-III compensation for current-mode, step-down dc/dc converters. The measurements also illustrate the gap between simulation and real world.

In addition, this report provides a quick and easy method to calculate the efficiency of a buck converter. These procedures provide accurate results and reduce the need to build and test the power supply to get the efficiency data. It is also helpful in the component selection for reaching the highest efficiency.

IMPORTANT NOTICE

Texas Instruments Incorporated and its subsidiaries (TI) reserve the right to make corrections, modifications, enhancements, improvements, and other changes to its products and services at any time and to discontinue any product or service without notice. Customers should obtain the latest relevant information before placing orders and should verify that such information is current and complete. All products are sold subject to TI's terms and conditions of sale supplied at the time of order acknowledgment.

TI warrants performance of its hardware products to the specifications applicable at the time of sale in accordance with TI's standard warranty. Testing and other quality control techniques are used to the extent TI deems necessary to support this warranty. Except where mandated by government requirements, testing of all parameters of each product is not necessarily performed.

TI assumes no liability for applications assistance or customer product design. Customers are responsible for their products and applications using TI components. To minimize the risks associated with customer products and applications, customers should provide adequate design and operating safeguards.

TI does not warrant or represent that any license, either express or implied, is granted under any TI patent right, copyright, mask work right, or other TI intellectual property right relating to any combination, machine, or process in which TI products or services are used. Information published by TI regarding third-party products or services does not constitute a license from TI to use such products or services or a warranty or endorsement thereof. Use of such information may require a license from a third party under the patents or other intellectual property of the third party, or a license from TI under the patents or other intellectual property of TI.

Reproduction of TI information in TI data books or data sheets is permissible only if reproduction is without alteration and is accompanied by all associated warranties, conditions, limitations, and notices. Reproduction of this information with alteration is an unfair and deceptive business practice. TI is not responsible or liable for such altered documentation. Information of third parties may be subject to additional restrictions.

Resale of TI products or services with statements different from or beyond the parameters stated by TI for that product or service voids all express and any implied warranties for the associated TI product or service and is an unfair and deceptive business practice. TI is not responsible or liable for any such statements.

TI products are not authorized for use in safety-critical applications (such as life support) where a failure of the TI product would reasonably be expected to cause severe personal injury or death, unless officers of the parties have executed an agreement specifically governing such use. Buyers represent that they have all necessary expertise in the safety and regulatory ramifications of their applications, and acknowledge and agree that they are solely responsible for all legal, regulatory and safety-related requirements concerning their products and any use of TI products in such safety-critical applications, notwithstanding any applications-related information or support that may be provided by TI. Further, Buyers must fully indemnify TI and its representatives against any damages arising out of the use of TI products in such safety-critical applications.

TI products are neither designed nor intended for use in military/aerospace applications or environments unless the TI products are specifically designated by TI as military-grade or "enhanced plastic." Only products designated by TI as military-grade meet military specifications. Buyers acknowledge and agree that any such use of TI products which TI has not designated as military-grade is solely at the Buyer's risk, and that they are solely responsible for compliance with all legal and regulatory requirements in connection with such use.

TI products are neither designed nor intended for use in automotive applications or environments unless the specific TI products are designated by TI as compliant with ISO/TS 16949 requirements. Buyers acknowledge and agree that, if they use any non-designated products in automotive applications, TI will not be responsible for any failure to meet such requirements.

Following are URLs where you can obtain information on other Texas Instruments products and application solutions:

Products		Applications	
Amplifiers	amplifier.ti.com	Audio	www.ti.com/audio
Data Converters	dataconverter.ti.com	Automotive	www.ti.com/automotive
DLP® Products	www.dlp.com	Communications and Telecom	www.ti.com/communications
DSP	dsp.ti.com	Computers and Peripherals	www.ti.com/computers
Clocks and Timers	www.ti.com/clocks	Consumer Electronics	www.ti.com/consumer-apps
Interface	interface.ti.com	Energy	www.ti.com/energy
Logic	logic.ti.com	Industrial	www.ti.com/industrial
Power Mgmt	power.ti.com	Medical	www.ti.com/medical
Microcontrollers	microcontroller.ti.com	Security	www.ti.com/security
RFID	www.ti-rfid.com	Space, Avionics & Defense	www.ti.com/space-avionics-defense
RF/IF and ZigBee® Solutions	www.ti.com/lprf	Video and Imaging	www.ti.com/video
		Wireless	www.ti.com/wireless-apps

Mailing Address: Texas Instruments, Post Office Box 655303, Dallas, Texas 75265
Copyright © 2010, Texas Instruments Incorporated